UC 20 a,f,g

WISC

UNIVERSITY OF WISCONSIN • MADISON, WISCONSIN

PLASMA PHYSICS

AXISYMMETRIC INSTABILITY IN A NONCIRCULAR TOKAMAK: EXPERIMENT AND THEORY

BY

B. Lipschultz, S.C. Prager, A.M.M. Todd, and J. Delucia

COO-2387-116 September 1979

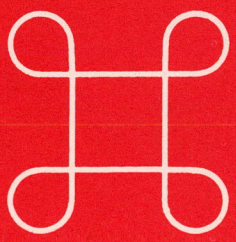

ONSIN

DISCLAIMER

NOTICE

Printed in the United States of America
Available from
National Technical Information Service
U. S. Department of Commerce
5285 Port Royal Road
Springfield, VA 22161

NTIS price codes
Printed copy: A03
Microfiche copy: A01

AXISYMMETRIC INSTABILITY IN A NONCIRCULAR TOKAMAK: EXPERIMENT AND THEORY

by

B. Lipschultz and S.C. Prager
University of Wisconsin, Madison, Wisconsin, 53706, U.S.A.

and

A.M.M. Todd and J. Delucia
Princeton Plasma Physics Laboratory, Princeton, New Jersey, 08544, U.S.A.

C00-2387-116

This is a preprint of a paper to be submitted for publication in Nuclear Fusion

September 1979

ABSTRACT

The stability of dee, inverse-dee and square crossection plasmas to axisymmetric modes has been investigated experimentally in Tokapole II, a tokamak with a four-null poloidal divertor. Experimental results are closely compared with predictions of two numerical stability codes--the PEST code (ideal MHD, linear stability) adapted to tokapole geometry and a code which follows the nonlinear evolution of shapes similar to tokapole equilibria. Experimentally, the square is vertically stable and both dee's unstable to a vertical nonrigid axisymmetric shift. The central magnetic axis displacement grows exponentially with a growth time~10^3 poloidal Alfvén times~ plasma L/R time. Proper initial positioning of the plasma on the midplane allows passive feedback to nonlinearly restore vertical motion to a small stable oscillation. Experimental poloidal flux plots are produced directly from internal magnetic probe measurements. The PEST code, ignoring passive feedback, predicts all equilibria to be vertically unstable with the square having the slowest growth. With passive feedback, all are stable. Thus experiment and code agree that the square is the most stable shape, but experiment indicates

that passive feedback is partially defeated by finite plasma resistivity. In both code and experiment square-like equilibria exhibit a relatively harmless horizontal instability.

displacements and analytic equilibria [4-12]. Recently nonlinear evolution of the instability has been followed numerically [13]. Axisymmetric displacement of dee and elliptical plasmas has been deduced in a few experiments from magnetic probes external to the plasma[14-17]. The plasma shape in these experiments has been inferred from comparison of these same external magnetic signals with output from equilibrium computer codes. The numerical modeling of the axisymmetric instability, cited above, has apparently not been specifically applied to any of these experiments; an unfortunate gap exists between a fairly well developed theory and experiments performed.

The purpose of this paper is twofold. First, to report direct experimental observation of the axisymmetric instability in dee, inverse-dee and square shaped cross sections. Second, to compare these experimental observations with a stability code written for the actual experimental geometry. This experiment has been performed in the Wisconsin Tokapole[18,19], a Tokamak with a four-null poloidal divertor. Experimental magnetic flux plots for the aforementioned range of equilibria are produced, from magnetic probe measurements in the plasma interior, in detail equivalent to that provided by computer calculations. Conclusions, as to growth rates and passive stabilization,

I. INTRODUCTION

The deleterious effect of impurities in tokamak plasmas has stimulated investigation of poloidal divertor configurations. The necessarily noncircular shape of these equilibria is also advantageous with respect to q^1 and β-limited MHD instabilities[2,3]. Unfortunately any deviation of an equilibrium from a circular shape may permit the plasma to be unstable to axisymmetric displacements, with toroidal mode number n=0. The circular shape is neutrally stable to these displacements. The poloidally asymmetric placement of shaping rings and walls necessary to establish a noncircular plasma shape in turn creates nonuniform attractions to the plasma current. The plasma, if perturbed, moves in the direction of the minimum in the accompanying poloidal field. Unlike kink and localized interchange modes, the axisymmetric instability cannot be controlled by increasing the toroidal field or reducing the plasma current.

Unfortunately, the conceptual simplicity of the axisymmetric instability does not translate to calculational simplicity. The importance of this mode has given rise to a fairly large amount of linear theory - mostly for idealized

can be drawn from the time evolution of these experimental flux plots and compared with two numerical codes which closely reflect the experimental machine. The PEST code[20], which has been adapted to the Tokapole machine geometry, predicts the linear stability . The effects due to external conductors are included by appropriate vacuum modifications[21,22]. A nonlinear time dependent code, PATENT[13,23], although in this paper applied to PDX[24] type equilibria only, provides qualitative stability predictions and modeling of the plasma shape as a function of time. Because of the wide seperation of time scales in this experiment (e.g. Alfvén, plasma and ring L/R times) many qualitative conclusions about passive stabilization can be drawn which are relatively machine independent. Qualitative comparison can also be made between experimental results and related models in the literature[19].

Several parameter variations are possible both experimentally and numerically. For example, proper positioning of the four field shaping rings allows equilibria to be varied from dee through square to inverse-dee shaped. The dee and inverse-dee are vertically unstable when not well centered on the machine midplane. When vertical stability is achieved, these shapes are still horizontally unstable. The square is vertically stable even

if not properly positioned. However, this shape is also horizontally unstable. Since the horizontal instability saturates it is less harmful than the vertical displacements exhibited in the dee and inverse-dee. The vertical movement continues unrestrained towards the x-point (poloidal field null on the separatrix). Predictions of the PEST code for relative stability of these equilibria agree with experiment. Experimentally, the magnetic axis can be positioned above ($\gtrsim$.03 minor radii), below or exactly on the midplane. In both the PATENT code and experiment the plasma is seen to correspondingly move up, down or oscillate about the midplane. Both experimentally and from the nonlinear code we find the growth of the instability to be exponential in time. Ideal MHD predicts the growth time, in the absence of external conductors, to be $\sim\tau_a$, the poloidal Alfvén time. Experimentally, vertical and horizontal growth times are $\sim 10^3 \tau_a$. Passive feedback apparently increases τ_g, the growth time, from τ_a to roughly the plasma L/R time. The effect of passive feedback from rings and walls is studied experimentally by changing the plasma resistivty and by varying the initial position of the magnetic axis. The instability growth time varies inversely with plasma resistivity. Stability can be numerically studied with or without rings or walls to evaluate their effect on passive stabilization.

Section II, after a machine description (II.A), describes the stability of various plasma cross sections (II.B), the effect of plasma resistivity (II.C) and initial plasma position (II.D). In Section III, after code descriptions (III.A), theoretical results are described with (III.B) and without (III.C) passive feedback. Experimental and theoretical results are discussed and compared in Section IV with a summary in Table I.

II. EXPERIMENTAL RESULTS

A. Machine Description

The Tokapole device[18], on which these experiments were performed, has a 50 cm. major radius square cross section (44 x 44 cm.) vacuum chamber. The vacuum magnetic flux plot is that of an octupole (fig. 1a), which provides vertical and horizontal fields to center the discharge. The octupole vacuum poloidal field is produced by inductively driving, through an iron core linking the toroid, four 5 cm. diameter copper toroidal rings. These rings can carry up to a total of 700 kA, and are each supported by three copper-beryllium rods. While the chamber is under vacuum the rings can be moved vertically ±5mm. by external means. When plasma current is driven toroidally through the octupole null, a tokamak with a four-null divertor is generated (fig. 1b).

Electrical characteristics are shown in figure 2. The current in an outer ring rises sinusoidally to 45 kA (fig. 2a). A 1 msec. pulse of 10 kW. 8.8 GHz microwaves is used for preionization (fig. 2b). The plasma current (fig. 2b also) is induced by the same source as the ring current. The value for the total toroidal plasma curent is inferred

from measurements of the ring current and loop voltage, at the wall, employing a simple model treating the plasma and rings as coupled inductors. The current inside the separatrix is also calculated from measured magnetic flux plots. The peak total plasma current is ~ 40 kA with ~ 4 msec pulse length (fig. 2b). The toroidal field is 3.2 kG at machine center, with capability of up to 8.5 kG. The vacuum toroidal loop voltage (fig. 2c) at machine center decays as a cosine to zero in ~ 3 msec and is then crowbarred. In the presence of plasma the loop voltage is depressed during current rise and enhanced during current decline due to the back EMF self-induced by the plasma current. Peak electron temperatures are ~ 100 eV surmised, with ~ 25% accuracy, from modeling of the time evolution of a set of impurity lines (e.g. OI-OVI). The electron density is $\sim 10^{13}$ cm^{-3} as measured by microwave interferometry. The ion temperature varies from 20-70 eV as determined by charge-exchange analysis and from the doppler broadening of He II.

B. Relative Stability of Dee, Inverse-dee and Square Equilibria

This experiment allows comparison of various plasma shapes in one machine under similar conditions. By varying the placement of the rings, which attract the plasma, the shape of the tokamak separatrix can be changed from dee to inverse-dee (figures 3a-c). If the inner rings are moved closer together, and thus nearer the plasma, the equilibrium is positioned slightly inward in major radius producing a dee (fig. 3a). An inverse dee (fig. 3b) is created by positioning the outer rings closer together. The intermediate case is a square plasma (fig. 3c). Previous experiments concerning noncircular tokamaks have deduced the plasma shape using external measurements such as winding currents, plasma current and edge magnetic fields, combined with computer modeling. All important data in this paper, such as flux plots, current density and electric field profiles are deduced from internal probe measurements.

The poloidal magnetic flux plot is produced by measuring the magnetic field, with a pickup loop .4x.5 cm., as a function of time on a 2 cm. square grid. Temperatures are sufficiently low that probes can be inserted into the

plasma with little observable effect on the axisymmetric instability. After locating the o-point (magnetic axis) in the experimental data, the flux surfaces are derived by integrating flux out from that point.

The time histories of these flux plots show that the dee and inverse-dee are unstable to a non-rigid vertical movement, along a line of sight from the magnetic axis to a ring (figure 4). The square is stable to this movement on the time scale of this experiment. For the vertically unstable shapes, a plot of the magnetic axis position, shown in figure 5, indicates that the vertical displacement increases exponentially with a growth time $\tau_g \sim 450$ μsec. $\tau_g \sim 10^3 \tau_a$, where τ_a is a poloidal Alfvén time calculated with a suitably averaged poloidal field. It is also interesting to note, and will be discussed later, that τ_g is much less than the resistive decay time of rings and walls (15 msec) and very close to the plasma L/R time (.5-2.0 msec).

We find that all these equilibria can be stabilized to vertical movement, on the time scale of this experiment, by precise positioning of the rings. After the vertical movement is stabilized there still remains a horizontal motion that is independent of the rise and fall of the plasma current. This horizontal instability occurs in the

square as well as the dee and inverse-dee. The direction of this motion depends strictly on which set of rings the inner plasma separatrix encircles. When the plasma "leans" on the outer (inner) set of rings the movement is towards increasing (decreasing) major radius. Growth times for this horizontal instability, like the vertical, are ~ $10^3\tau_a$.

C. Effect of Plasma Resistivity

The role of passive stabilization could be all important to this instability and perhaps in practice eclipse distinctions based on plasma shape. Since the rings are inductively driven, there are no external circuit connections between them. Thus they are free to independently respond to the plasma motion. However, the efficacy of passive feedback, arising from induced image currents flowing in external conductors and plasma, is limited by the finite resistivity of the elements involved. Wooton et. al.[14] found the growth of an axisymmetric instability, in TOSCA, slowed down by the resistive decay of induced stabilizing currents in its walls and external field shaping coils. Theoretically, the equivalent prediction has been made[8,13]. However, all these calculations assume an ideal, infinitely conducting plasma. In the Tokapole experiment the finite plasma resistivity (L/R time ~ 1 msec) is the major contributor to the damping of induced stabilizing currents. The rings and walls in this experiment have a much longer resistive decay time (15 ms.) than the plasma. Indeed, instability growth occurs on the plasma L/R time scale.

To address this issue we changed the plasma resistance

while keeping the plasma inductance and shape relatively constant. Resistivity profiles are obtained from current and electric field profiles.

The loop voltage, or electric field, spatial profile is measured with a 4mm. by 50 cm. loop of wire which encloses poloidal flux between a given location and the wall (machine floor or ceiling). Measurement of this flux and the loop voltage at the wall yields the loop voltage at that given location, if axisymmetry is assumed.

Current density profiles are obtained from measured flux plots. The current enclosed by a particular flux surface can be calculated by integrating $\underline{B} \cdot \underline{dl}$ around the circumference. By knowing the total current enclosed by a number of flux surfaces a current density profile can be obtained up to the separatrix or last closed flux surface inside the experimental data grid. Examples of typical current, electric field and corresponding resistivity profiles are shown in figures 6 and 7.

The resistivity profile was varied in two ways: First, by lowering the toroidal magnetic field which lowers the plasma current. Second, by puffing Ar gas, in addition to the normal H_2, to increase Z_{eff} directly. In either case

the electric field profile stayed relatively constant while the current channel width and magnitude decreased as shown for the first method in figures 6 & 7. In the particular case shown the instability onset occurred at ~ 2 ms. Such large resistance changes were necessary in order to exceed the 20% uncertainty in the measurements involved. The shape of the equilibrium was verified to be approximately the same as the unmodified case, at instability onset, by examination of the magnetic flux plots. The plasma inductance remained relatively unchanged (<10%) indicating that the decrease in the L/R time of the plasma was mainly due to the change in plasma resistance. As seen from figures 5 & 8, τ_g decreased by at least a factor of 2 for either lower toroidal field or Ar puffing. Correspondingly, figure 7 indicates the plasma resistance increased by roughly a factor of two. This result is consistent with the general statement that τ_g is proportional to the minimum resistive decay time in the passive stabilization circuit. In our specific case τ_g is inversely proportional to the plasma resistance.

D. Effect of the Initial Plasma Position

It is important to be able to adjust the initial vertical position of the plasma in order to investigate the marginal stability case, assess the difficulty of passive stabilization and check the vertical symmetry of the machine. Through ring movement we can position the magnetic axis, initially, up to .1 minor radii above or below the midplane. We can also, for dee and inverse-dee equilibria, precisely position the plasma z-symmetrically such that it appears vertically stable.

When an otherwise unstable shape is stabilized through proper positioning, the magnetic axis exhibits an oscillatory motion (fig. 9a) about the midplane with period approximately equal to the growth time of the unstable cases. For small vertical displacements of the initial magnetic axis position from the midplane, this same oscillatory motion is superposed upon a steady vertical movement (fig. 9b). For still larger displacements of the initial magnetic axis position, the oscillatory motion disappears and the movement is strictly exponential (fig. 5). Thus we see that increasing the initial displacement leads to faster growth. Machine vertical symmetry is

verified by positioning the initial magnetic axis above or below the midplane and observing upward or downward motion respectively.

III. THEORY

A. Code Description

Quantitative comparison of the experimental evolution of magnetic flux plots with published analytic and numerical examples is not possible. Experimental equilibria are not well fitted by analytic models (e.g. Solov'ev[25] or Rebhan[5,6]). Also, for the most part, these studies evaluate stability limits as opposed to relative growth rates, which can be important in the presence of passive stabilization. Two numerical stability codes have been used here to evaluate the stability of a broad range of equilibria for comparison with experiment. The PEST[20] code has been adapted to Tokapole geometry so that the stability of our experimental equilibria can be accurately evaluated. The PATENT code[23], although applicable to PDX[24] equilibria only, may be used to follow the nonlinear development of shapes similar to those of the Tokapole.

PEST is an ideal MHD linear stability code. Eigenvalues and modes are calculated by extremizing the Lagrangian of a given equilibrium configuration. The version of PEST used in these calculations employs a vacuum energy formulation that includes the inductive energy of

arbitrary conducting elements[21,22]. These elements may be coils, rings, plates or any other conducting members embedded in the vacuum region between the plasma and the wall, which can be removed to infinity. Ideal MHD instabilities have growth times τ_a, on which time scale such elements are perfect conductors. Thus the growth rates obtained reflect passive stabilization by the induced currents, and cannot predict mode behavior as these currents resistively decay, or when the perturbation becomes sufficiently large as to violate linear theory.

PATENT is an ideal MHD, 2-D, time dependent code that follows the evolution of the plasma seperated from the vacuum region by a sharp boundary. Magnetic flux coordinates are used whereby the vacuum-plasma interface is well defined. This, combined with stepping through time, allows one to watch the plasma shape deform as the instability grows.

B. Results Without Passive Feedback

The PEST code is used to evaluate the axisymmetric stability of a range of Tokapole and PDX equilibria (figures

10-12) from inverse-dee to square to dee. Comparison of Tokapole and PDX results can be used to determine the generality of the experiment. Stability may be calculated with the rings and walls either included or excluded to assess the role of passive stabilization. The deeness of the equilibria may be described by fitting the flux surface just inside the separatrix by the expression introduced by Rebhan[5]:

$$e^2/A^2 = e^2(R-1)^2+(1+\tau_3^2)z^2-2A\tau_3(R-1)z^2-\tau_4A^2(R-1)^2z^2$$

where e is the ellipticity, τ_3 is a measure of the triangularity or deeness, τ_4 is a measure of rectangularity and A is the aspect ratio. This expression is useful because it allows a description of dee, inverse-dee, elliptical as well as square shaped cross sections. The dependence of the instability growth rate on deeness (τ_3) may now be observed. Ignoring the presence of rings and walls, figures 10 and 11 show that the square is more stable, vertically, than the dee or inverse-dee, which have roughly equal growth rates, for both Tokapole and PDX equilibria. These machines are quite different in geometry and size. In addition, the Tokapole has a flatter current profile than the parabolic shape predicted for PDX. It

appears that the relative stability of different shaped cross sections is fairly machine independent.

The growth rates for PDX calculated by PATENT (figure 11) agree well with PEST. Using PATENT, the motion of the magnetic axis may be observed for different initial perturbations. It is seen (fig. 13) that if the axis is initially .02 minor radii above the midplane the plasma moves unstably upward. Equivalent positioning of the axis below the midplane produces downward motion. Typical initial and final pictures of the equilibrium are shown in figure 14. The growth is exponential for excursions well into the nonlinear regime. Growth rates increase as the initial position of the magnetic axis is moved farther from the midplane (fig. 15). For an initial vertical position of the magnetic axis on the midplane, the axis oscillates about that starting point.

The effect of the toroidal field on instability growth was found to be minimal. An order of magnitude difference in the toroidal field produced only a .5% change in growth rate; stability was enhanced for inverse-dee's ($\tau_3>0$), degraded for dee's ($\tau_3<0$). This difference is perhaps related to the $\underline{J}_{pol}\times\underline{B}_{tor}$ force which points outward from the plasma center. As the unstable dee ($\tau_3<0$) moves inward in

major radius to higher B_{tor}, the force increases thereby encouraging unstable motion. For the inverse-dee ($\tau_3>0$) the motion is outward and the effect of the toroidal field is opposite.

Stability to horizontal axisymmetric displacements of Tokapole and PDX equilibria was studied using PEST. For Tokapole equilibria, the square and other shapes of small $|\tau_3|$, were found to be horizontally unstable with the square having the highest growth rate (fig. 12). During horizontal motion the midplane forces due to the vertical field are stabilizing wheras the vertical extremities experience the destabilizing attraction to the rings. Therefore local stability criteria are insufficient; all the forces over the entire plasma cross section must be considered. The decay index[26] applied to horizontal stability only describes the stabilizing influence on the midplane. The dee's, which are more heavily weighted in area towards the stabilizing midplane, are relatively more stable than the square. Examination of figure 12 reveals the dee to be relatively more stable than the inverse-dee to horizontal motion. This difference is most likely due to the toroidal expansive force of the plasma current. For sufficiently large $|\tau_3|$

both Tokapole and PDX equilbria were found to be horizontally stable.

C. Results With Passive Feedback

Both codes can be used to assess the role of passive conductors surrounding the plasma. In the case of the PEST code, any combination of conductors (walls and/or rings) can be included and their effect on the linear growth is found by evaluating the inductive contribution to the energy principle of Bernstein et al.[21,22,27]. Figure 10 shows the effect of adding either rings or walls. In the presence of both walls and rings all Tokapole equilibria studied are stable except those of extreme triangularity. As can be seen from this same figure, adding conductors has a greater effect on the square than on other plasma cross sections. This may be due to the square being in closer proximity to all four rings or walls than shapes of larger $|\tau_3|$. The stabilizing effect of the rings exceeds that of the walls since the rings are closer to the plasma. The PATENT code yielded similar results when used to evaluate the effect of passive feedback due to rings.

IV. DISCUSSION AND SUMMARY

Previous experimental work[14-17] on the axisymmetric instability in noncircular tokamaks has, for the most part, inferred gross plasma motion from signals external to the plasma. Experimental results were compared with related theories in the literature through such parameters as ellipticity and/or averaged decay index, derived by modeling the plasma current as a filament[26]. In this experiment we can accurately observe the motion of the poloidal magnetic flux surfaces and the time evolution of internal parameters (J,q,E) through internal measurements. This experimental data is carefully compared to theoretical predictions of PEST, applied to this specific machine. The plasma cross section is characterized by ellipticity, triangularity and rectangularity parameters. A second code, PATENT, follows the nonlinear time development. This code is only applied to PDX geometry with shapes similar to Tokapole equilibria. Similar results, by PEST, for the two different machine geometries indicates our results are fairly machine independent.

Linear theory predicts that, in the absence of passive stabilization, all experimental equilibria are vertically

unstable on the MHD time scale (τ_a) . However, the square is more stable than the dee or inverse-dee. This is consistent with the dee's being poloidally more asymmetric than the square; that is, the radius of curvature of the magnetic surface near the x-point is smallest for the dee's. Furthermore, only square-like equilibria are horizontally unstable. With the addition of passive feedback from rings and walls all equilibria are predicted to be stabilized with the greatest influence exerted by the rings. An experimental picture emerges in close agreement with theory, with modifications to account for the finite plasma resistivity limitation to the passive feedback. When the experimental plasma is z-symmetric both inside and outside dee's oscillate on the plasma resistive time scale. Thus, these equilibria are linearly unstable, as in theory without conductors, but are nonlinearly restored by passive feedback to a stable oscillation. Passive feedback does not linearly stabilize the equilibria; i.e. the plasma is displaced a finite amount before nonlinear feedback occurs. The complete stabilization of this mode by passive feedback, that the ideal MHD PEST code predicts, is not observed in the dee's since the finite plasma resistivity causes damping of the induced stabilizing currents in the rings, plasma and walls. The square appears entirely stable vertically,

implying that passive feedback is more effective for this shape as is also indicated theoretically in figure 10.

All evidence, both experimental and theoretical, indicates that the square is more stable than both dee's, which have similar stability properities. If the initial vertical position of the magnetic axis of both dee's is experimentally positioned above (below) the midplane they are linearly unstable. However, passive feedback is unable to reverse the vertical motion and the displacement grows exponentially with a growth time again on the order of the plasma L/R time (resistive decay time). Experimentally the square is vertically stable even when positioned away from the midplane. The form of the vertical displacement of the dee's seen experimentally (fig. 4) or in the PATENT code (fig. 14) is a non-rigid deformation in the direction of the separatrix x-point. Also, in both this code and experiment, the growth rate increases as the magnetic axis is positioned further above the midplane.

In the absence of vertical movement, a steady horizontal motion is experimentally evident. As the plasma travels horizontally it becomes increasingly dee-shaped (increasing $|\tau_3|$) and eventually becomes vertically unstable. Indeed, PEST predicts this same horizontal

instability for the square and other shapes of small $|\tau_3|$ (fig. 12). Thus, the vertically stable square, radially centered thru active feedback, might prove to be a favorable configuration.

A crucial factor absent in the codes used here, and in all published calculations, is the finite plasma resistivity. Seki[8] and Jardin[13] discuss only the finite conductivity of the external conductors. In our experiment the plasma resistive decay time may impose a bound on the instability growth time. When the plasma resistance is experimentally doubled, the instability growth rate also doubled. The correlation is not precise. Although the plasma shape remains approximately the same, a 1.5 cm. shrinkage in the plasma minor radius accompanies the resistance change. However, modeling of the effect of this change on the instability growth by PEST indicates that the minor radius decrease causes only a 4% increase in growth rate. The experimental and theoretical results of this paper are summarized in table I.

Finally, the results presented here are not peculiar to the Tokapole machine or geometry for three reasons. Firstly, the Tokapole machine is up-down symmetric since the plasma shows no vertical preference in it's motion. When

initially positioned slightly above (below) the midplane the unstable motion is upward (downward). When centrally positioned it oscillates. Secondly, qualitative comparison of PEST predictions for Tokapole and PDX are very similar despite obvious machine differences. Thirdly, the wide separation of the poloidal Alfvén, growth and ring L/R times ($\tau_g \sim \tau_{L/R(plasma)} \sim .05\ \tau_{L/R(rings)} \sim 10^3 \tau_a$) clearly indicates the determining factors of the growth rate.

Acknowledgements

We are indebted to Dr. S.C. Jardin for his help in using the PATENT code as well as to Dr.'s J.C. Sprott, R.S. Post and D.W. Kerst for their valuable comments.

Also, we would like to thank T. Osborne for assistance with flux plots, T. Lovell and his staff for technical assistance.

This work was supported by the U.S. Department of Energy.

REFERENCES

[1]Wesson, J.A., Nucl. Fusion 18 (1978) 87.

[2]Todd, A.M.M., Manickam, J., Okabayashi, M., Chance, M.S., Grimm, R.C., Greene, J.M., & Johnson, J.L., Nuclear Fusion 19 (1979) 743.

[3]Dobrott, D.R., & Miller, R.L., Phys. of Fluids 20 (1977) 1361.

[4]Rebhan, E., Nucl. Fusion 15 (1975) 277.

[5]Rebhan, E. and Salat A., Nucl. Fusion 16 (1976) 805.

[6]Rebhan, E. and Salat A., Nucl. Fusion 18 (1978) 1431.

[7]Fukuyama, A., Seki, S., Momota, H., Itatani, R., Japanese Journal of Applied Physics 14 (1975) 871.

[8]Seki, S., Momota, H., Itatani, R., Journal of Phys. Soc. of Japan 36 (1975) 1667.

[9]Bernard, L.C., Berger, D., Gruber, R., & Troyon, F., Nucl. Fusion 18 (1978) 1331.

[10]Rosen, M.D., Phys of Fluids 18 (1975) 482.

[11]Okabayashi, M. and Sheffield, G., Nucl. Fusion 14 (1974) 263.

[12]Becker, G. and Lackner, J., Plasma Physics and Controlled Nuclear Fusion Research (IAEA,Tokyo,1977) Vol. 1, 401.

[13]Jardin, S.C., Phys. of Fluids 21 (1978) 395.

[14]Wooton, A.J., Nucl. Fusion 18 (1978) 1161.

[15]Sakurai, K., Nakamura, K., Kuzushima, T., Tanaka, Y., & Okuda, T., J. of Phys. Soc. of Japan 43 (1977) 731.

[16]Cima, G., Robinson, D.C., Thomas, C.L., Wooton, A.J., Plasma Physics and Controlled Nuclear Fusion Research (IAEA, Tokyo, 1977) Vol. 1, 335.

[17]Toyama, P., Inoue, S., Itoh, K., Iwahashi, A., Kaneko, H., et al., ibid. 323.

[18]Biddle, A., Dexter, R., Groebner, R., Holly, D., Lipschultz, B., et al., Nuclear Fusion (in press).

[19]Lipschultz, B., Prager, S.C., Osborne, T.H., Sprott, J.C., & Phillips, M., Physical Review Letters 43 (1979) 36.

[20]Grimm, R.C., Greene, J.M., Johnson, J.L., in Methods in Computational Physics, Vol. 16(Killeen, J., Ed.) Academic Press, New York (1976) 253.

[21]Dewar, R.L., Nucl. Fusion 18 (1978) 1541.

[22]Todd, A.M.M., 'Passive Stabilization in a Linear Stability Code', submitted to Journal of Computational Physics.

[23]Jardin, S.C., Johnson, J.L., Greene, J.M., Grimm, R.C., Journal of Computational Physics 29 (1978) 101.

[24]Meade, D.M., Furth, H.P., Rutherford, P.H., & Seidl, F., Plasma Physics and Controlled Nuclear Fusion Research (IAEA, Vienna, 1975) Vol. 1, 605.

[25]Solov'ev, L.S., Zh. Eksp. Teor. Fiz. 53 (1967) p. 626; Soviet Physics - JETP 26 (1968) 400.

[26]Yoshikawa, S., Physics of Fluids 7 (1964) 268.

[27]Bernstein, I.B., Frieman, E.A., Kruskal, M.D., & Kulsrud, R.M., Proc. Royal Society (London) 244A (1958) 17.

FIGURE AND TABLE CAPTIONS

Fig. 1. Numerical poloidal flux plots (major axis to left). (a) Without plasma. (b) With plasma. Each tic mark indicates 2 cm.

Fig. 2. Electrical characteristics. Time in msec. is given on the abscissa. (a) Current in an outer ring as a function of time. Also shown is a 10 kW, 8.8 Ghz, 1 ms. microwave preionization pulse. (b) Plasma current. (c) Loop voltage at machine center with and without plasma.

Fig. 3. Experimental flux plots mapped out with magnetic probes. Only the area inside the separatrix is shown. Each tic mark indicates 2 cm. (a) Dee. (b) Inverse-dee. (c) Square.

Fig. 4. Time evolution of the experimental flux plot for (a) inverse-dee & (b) square. The dee evolves similarly to inverse-dee.

Fig. 5. Distance travelled by the magnetic axis as a function of time. Uncertainty in distance travelled is 1-2 mm. 100 μsec = 500 poloidal Alfvén times.

Fig. 6. Spatial profiles at 2.0 msec. (a) Current density for two values of toroidal field. The electric field profiles for both values are similar; only one is shown. (b) Resistivity calculated from electric field and current in (a). The separatrix is at a minor radius of 6 cm.

Fig. 7. Spatial profiles at 2.6 msec. (a) Current density and electric fields for two values of toroidal field. (b) Resistivity calculated from profiles in (a).

Fig. 8. Distance travelled by magnetic axis as a function of time for the two methods of raising the plasma resistivity; lowering the toroidal field and puffing in Ar gas in addition to the usual H_2. Movement of the magnetic axis in an unmodified case is shown in fig. 5.

Fig. 9. Distance travelled by magnetic axis as a function of time for different initial positions. (a) Initial position on the midplane. (b) Initial position slightly above the midplane (3-5 mm.). When initially positioned an equivalent amount below the midplane identical downward motion is observed. The case of initial position further still above the midplane (5-10 mm.) is shown in fig. 5.

Fig. 10. Theoretical vertical growth rates vs. τ_3, as predicted by PEST, for the Tokapole. Three cases are shown: X - Without passive stabilization. 0 - Only rings included. □ - Only walls included. Square, dee and inverse-dee shapes are described by $\tau_3=0$, <0 & >0 respectively. Including rings and walls completely stabilizes all shapes other than extreme $|\tau_3|$.

Fig. 11. Theoretical vertical growth rates vs. τ_3 for PDX as predicted by the PEST and PATENT codes without passive stabilization.

Fig. 12. Theoretical horizontal growth rates vs. τ_3 for the Tokapole, as predicted by PEST, without passive stabilization.

Fig. 13. Predictions by PATENT for vertical position of the magnetic axis as a function of time. Initial perturbation in this case is .02 minor radii.

Fig. 14. Theoretically predicted (PATENT) deformation of the plasma shape for PDX. (a) Initial equilibrium. (b) t~ 100 toroidal Alfven times.

Fig. 15. Theoretical predictions of the non-linear code (PATENT) for growth rate as a function of perturbation. Note that the growth rate $\rightarrow 0$ for zero perturbation.

Table I. Comparison of experiment and theory as predicted by the numerical stability codes.

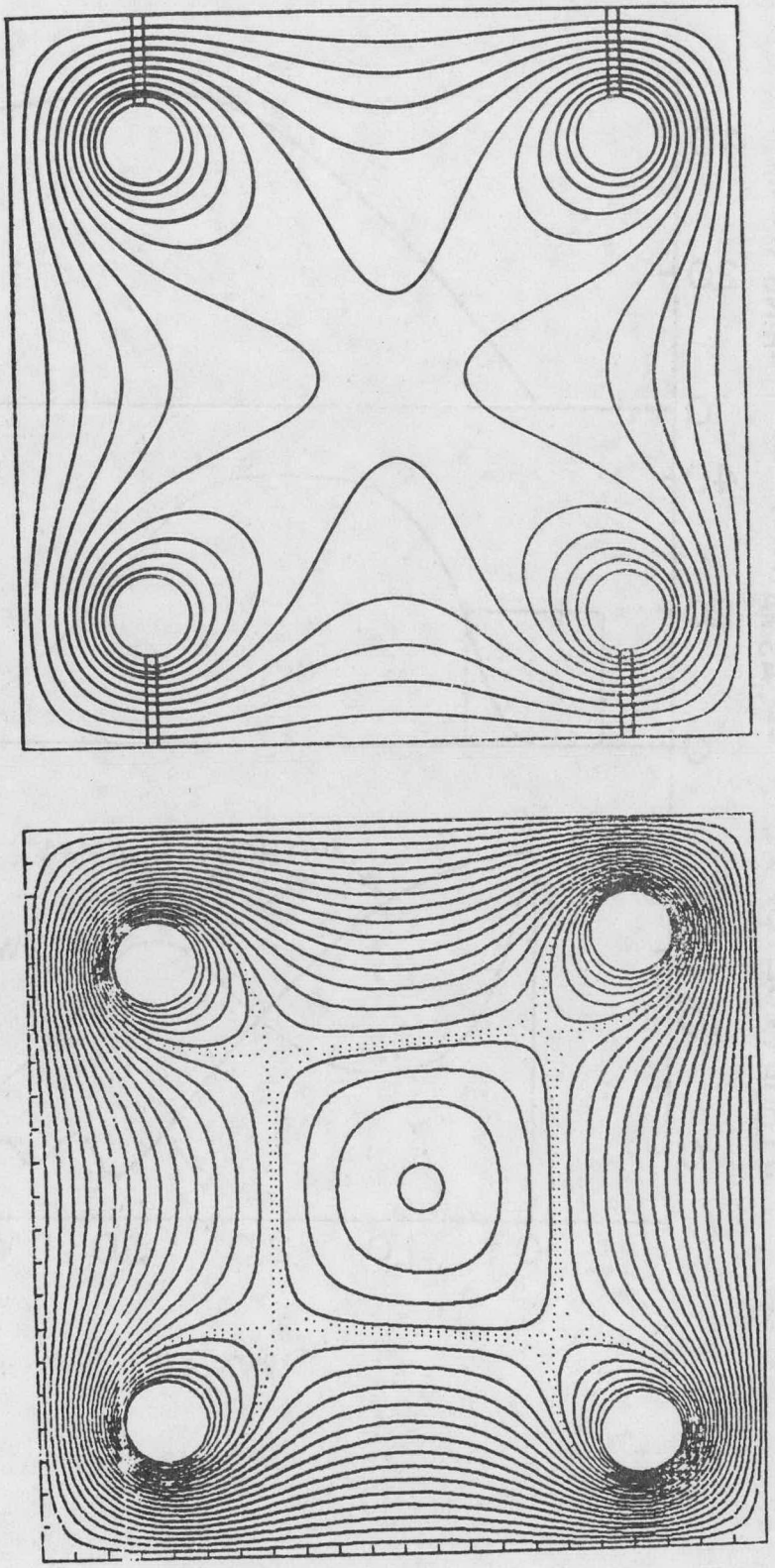

Figure 1

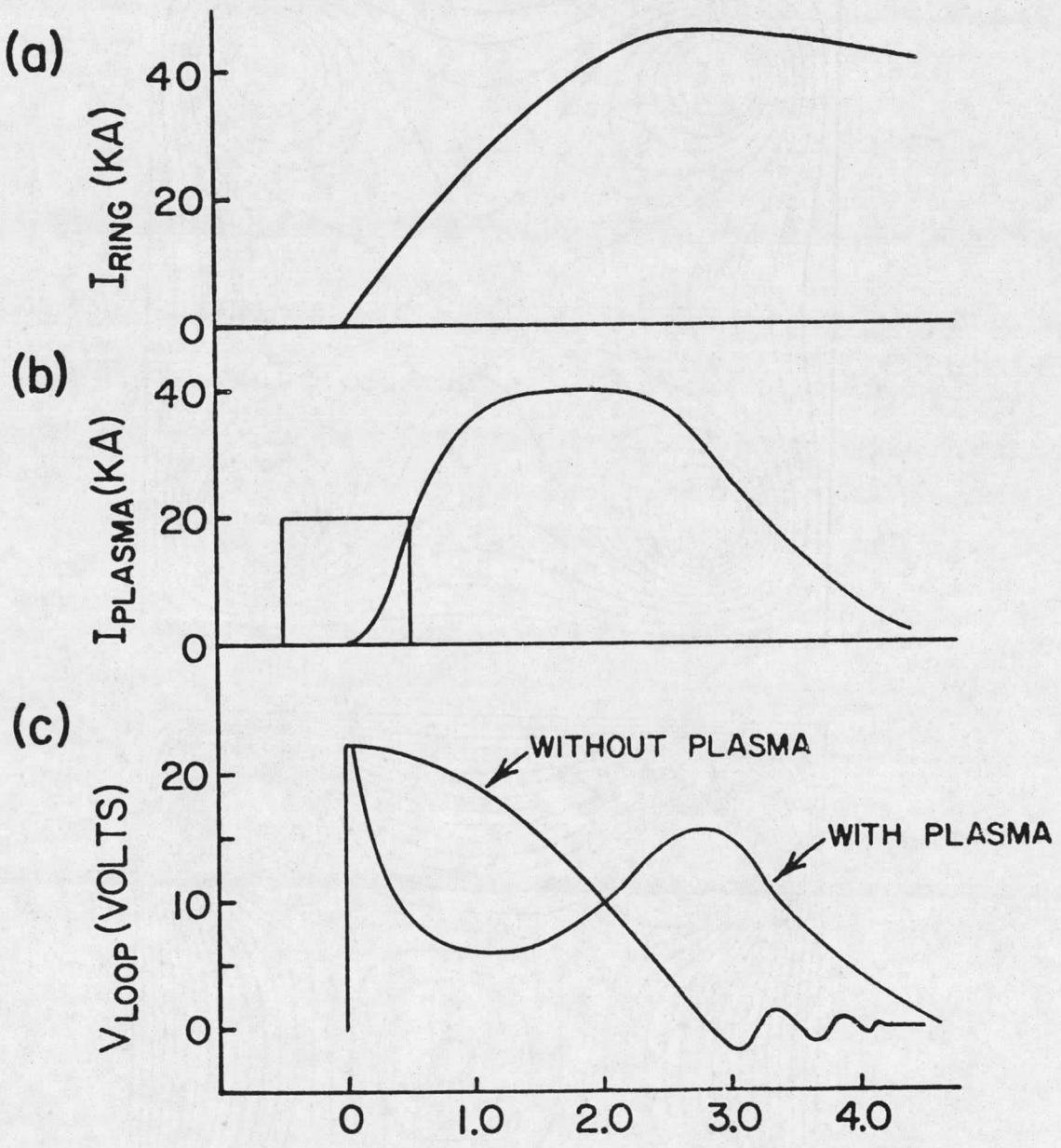
(a)
40
20
0
I_{RING} (KA)
(b)
40
20
0
I_{PLASMA}(KA)
(c)
20
10
0
V_{LOOP} (VOLTS)
WITHOUT PLASMA
WITH PLASMA
0
1.0
2.0
3.0
4.0

Figure 2

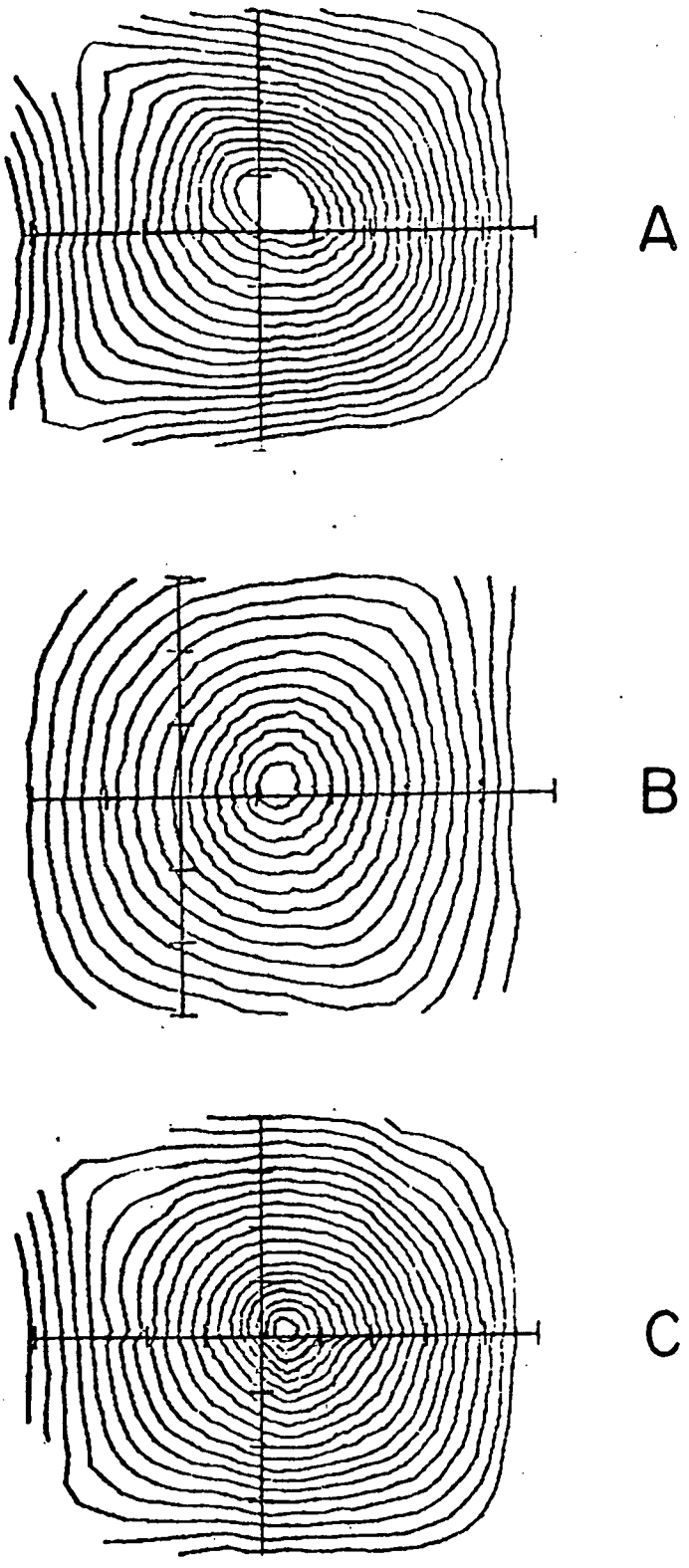

Figure 3

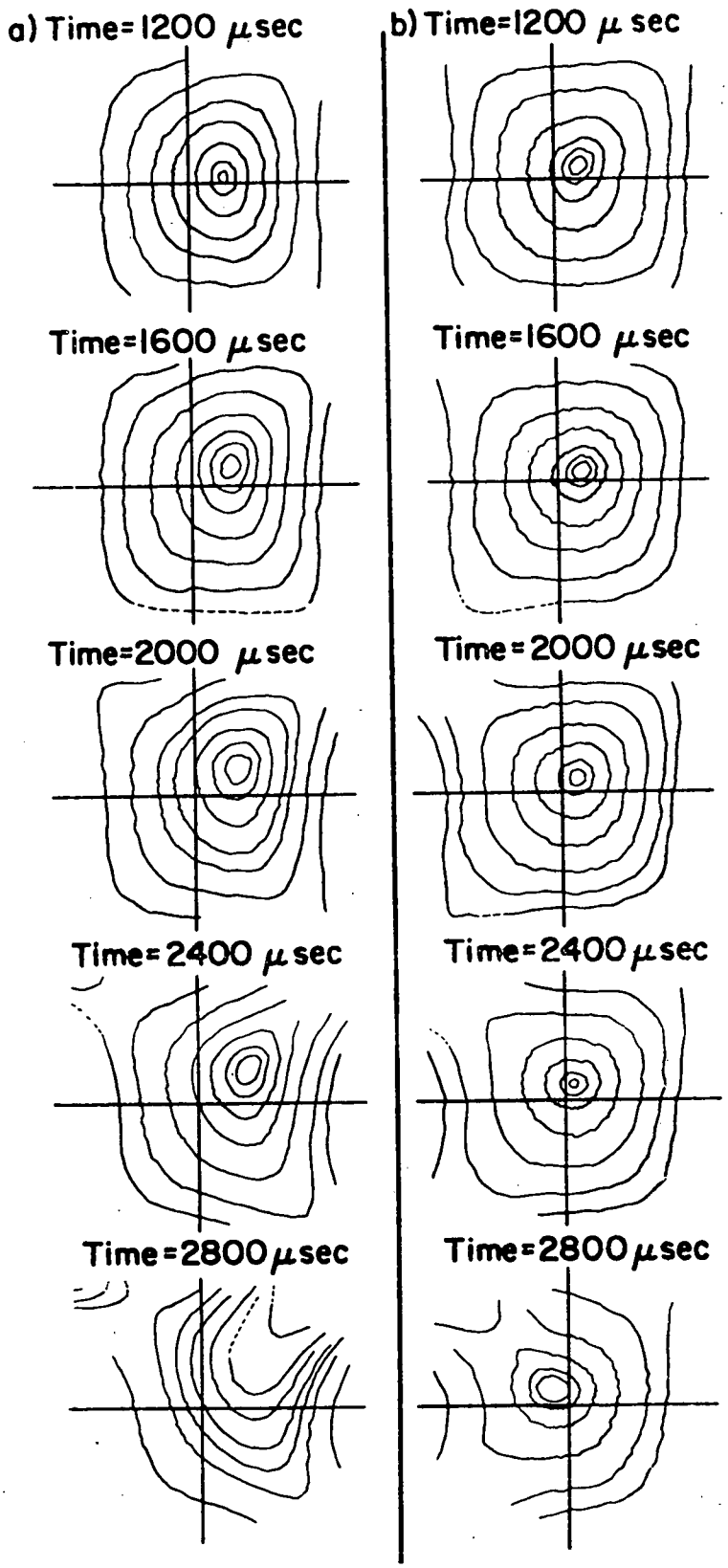
a) Time=1200 μsec
b) Time=1200 μ sec
Time=1600 μsec
Time=1600 μsec
Time=2000 μsec
Time=2000 μsec
Time=2400 μsec
Time=2400 μsec
Time=2800 μsec
Time=2800 μsec

Figure 4

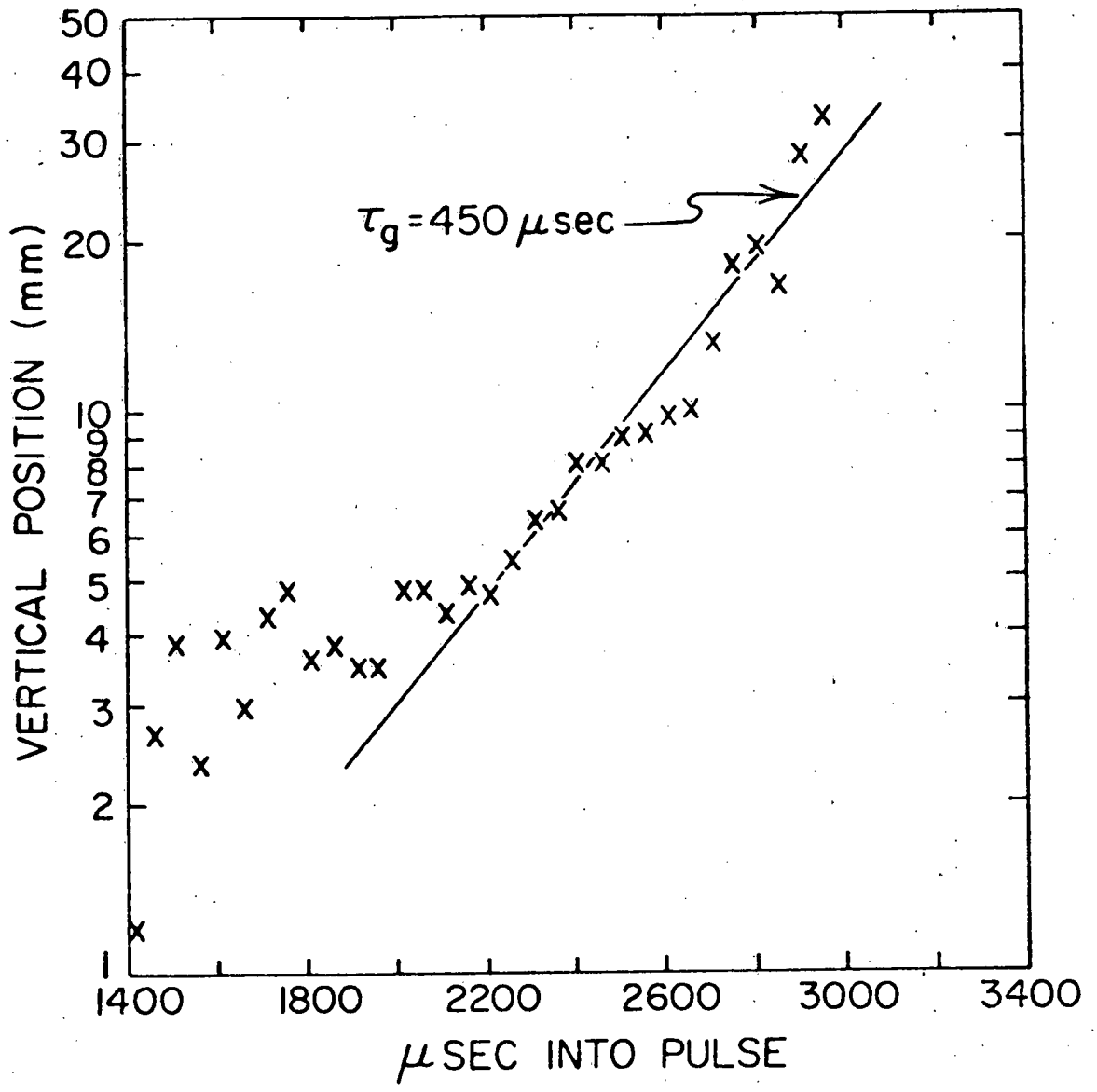
50
40
30
20
10
9
8
7
6
5
4
3
2
1
VERTICAL POSITION (mm)
τ_g = 450 μsec
1400
1800
2200
2600
3000
3400
μSEC INTO PULSE

Figure 5

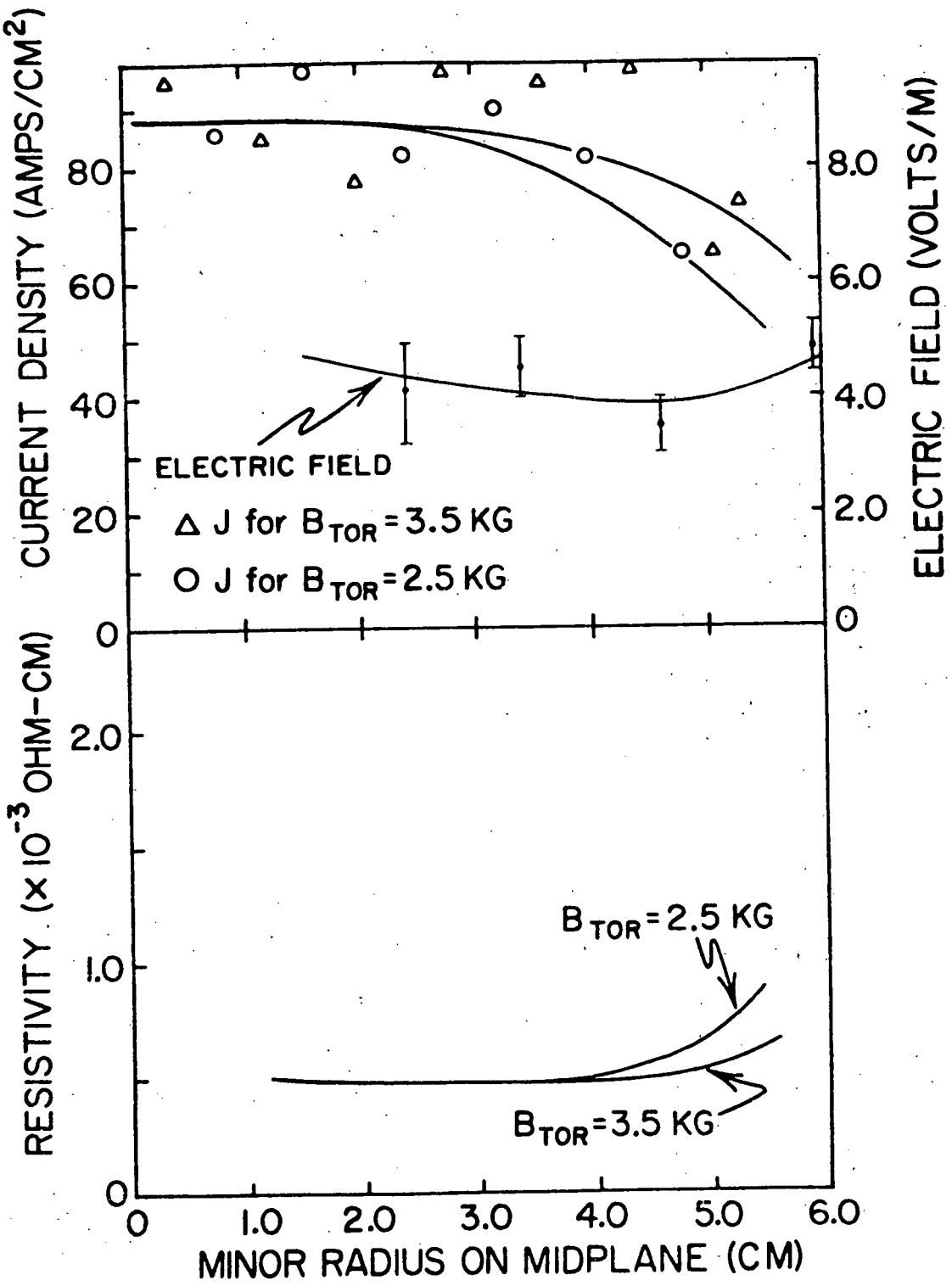
CURRENT DENSITY (AMPS/CM²)
ELECTRIC FIELD (VOLTS/M)
RESISTIVITY (X 10⁻³ OHM-CM)
MINOR RADIUS ON MIDPLANE (CM)
ELECTRIC FIELD
Δ J for B_TOR = 3.5 KG
O J for B_TOR = 2.5 KG
B_TOR = 2.5 KG
B_TOR = 3.5 KG
0
20
40
60
80
0
2.0
4.0
6.0
8.0
0
1.0
2.0
3.0
4.0
5.0
6.0
0
1.0
2.0

Figure 6

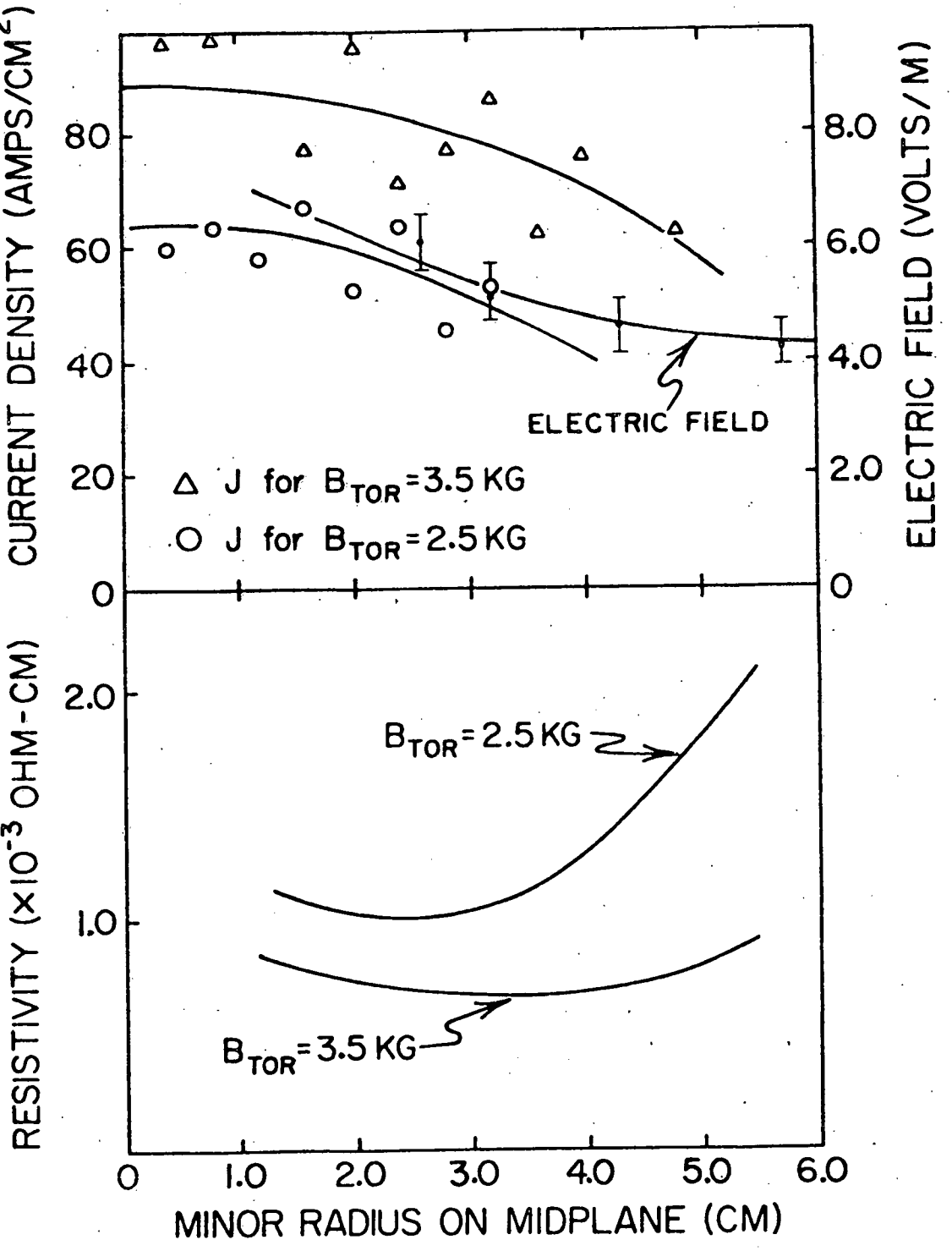
CURRENT DENSITY (AMPS/CM^2)
ELECTRIC FIELD (VOLTS/M)
80
60
40
20
0
8.0
6.0
4.0
2.0
0
ELECTRIC FIELD
△ J for B_{TOR}=3.5 KG
○ J for B_{TOR}=2.5 KG
RESISTIVITY (×10^{-3} OHM-CM)
2.0
1.0
B_{TOR}=2.5 KG
B_{TOR}=3.5 KG
0
1.0
2.0
3.0
4.0
5.0
6.0
MINOR RADIUS ON MIDPLANE (CM)

Figure 7

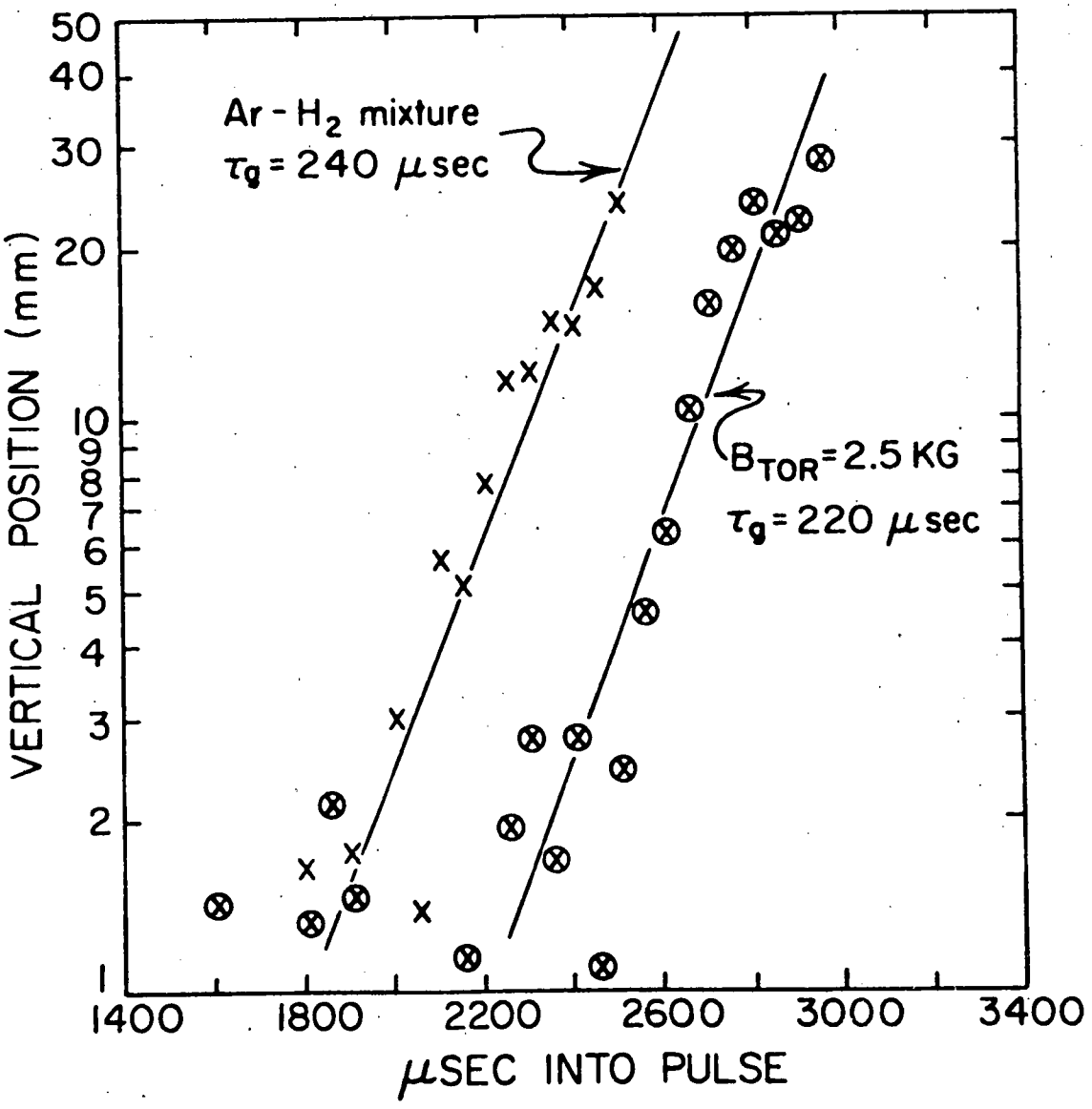
Ar - H2 mixture
τg = 240 μsec
BTOR = 2.5 KG
τg = 220 μsec
VERTICAL POSITION (mm)
μSEC INTO PULSE
50
40
30
20
10
9
8
7
6
5
4
3
2
1
1400
1800
2200
2600
3000
3400

Figure 8

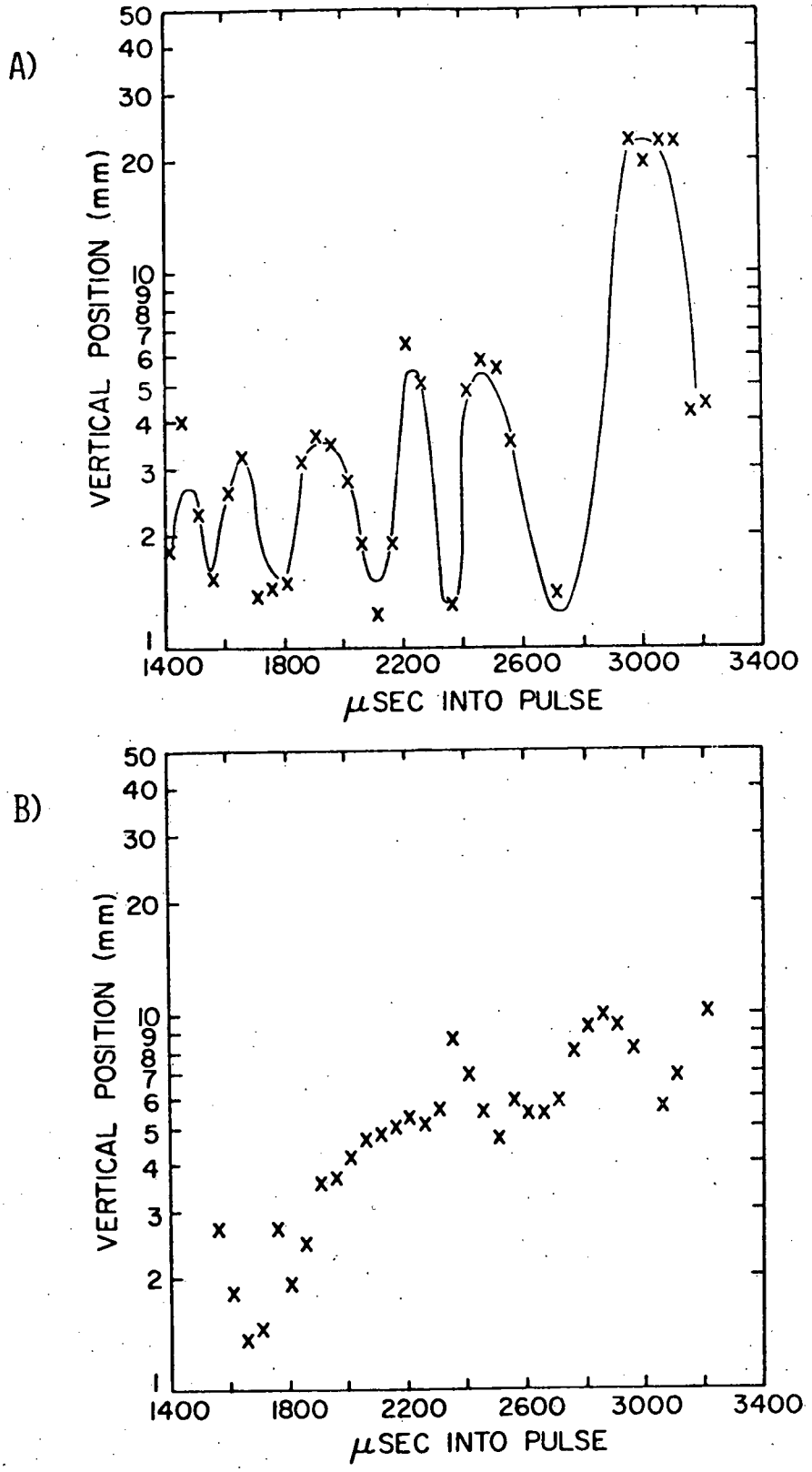
A)
B)
VERTICAL POSITION (mm)
μSEC INTO PULSE
50
40
30
20
10
9
8
7
6
5
4
3
2
1
1400
1800
2200
2600
3000
3400

Figure 9

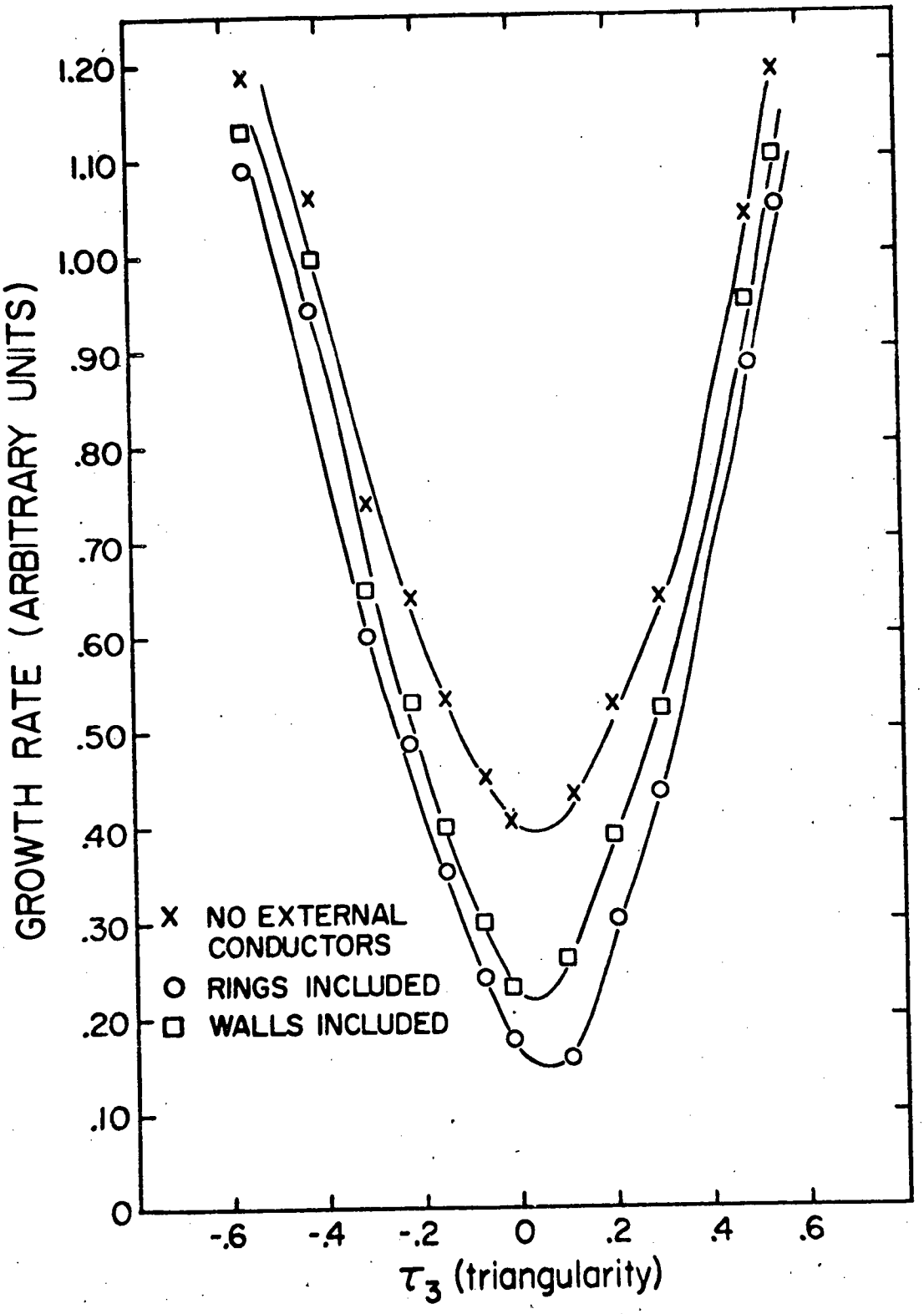
GROWTH RATE (ARBITRARY UNITS)
1.20
1.10
1.00
.90
.80
.70
.60
.50
.40
.30
.20
.10
0
-.6
-.4
-.2
0
.2
.4
.6
τ_3 (triangularity)
X NO EXTERNAL CONDUCTORS
O RINGS INCLUDED
□ WALLS INCLUDED

Figure 10

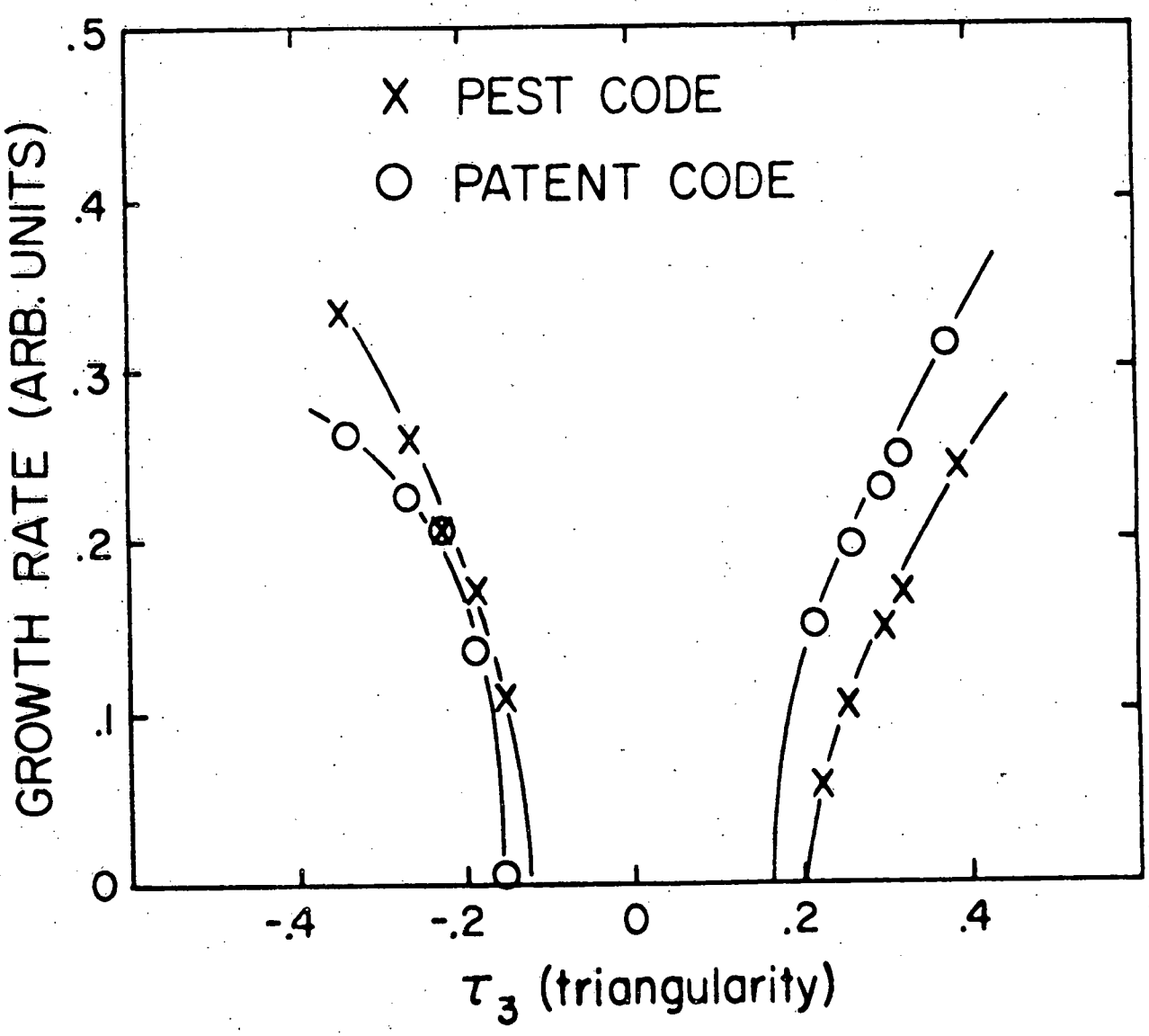
X PEST CODE
O PATENT CODE
GROWTH RATE (ARB. UNITS)
.5
.4
.3
.2
.1
0
-.4
-.2
0
.2
.4
τ_3 (triangularity)

Figure 11.

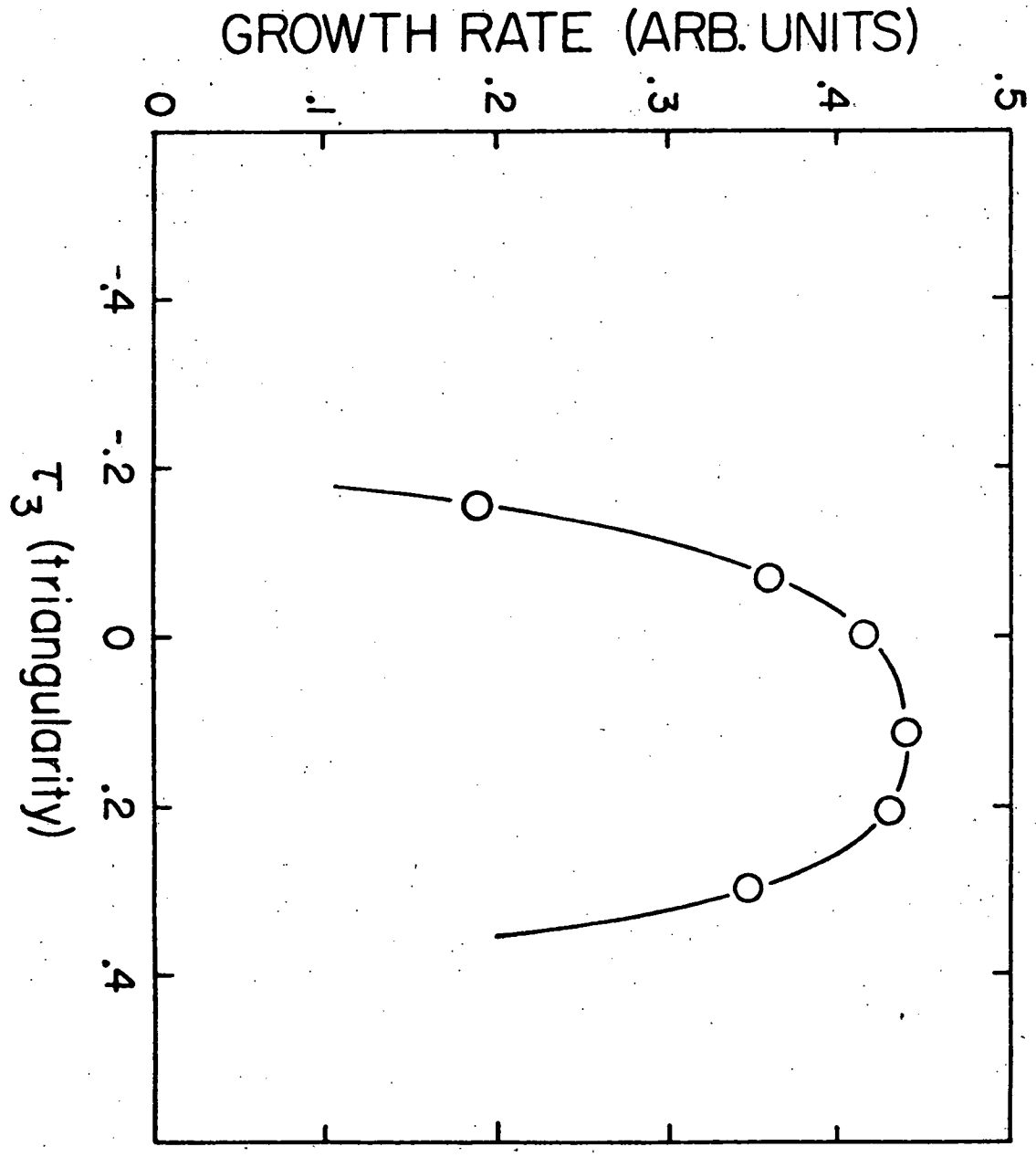

Figure 12

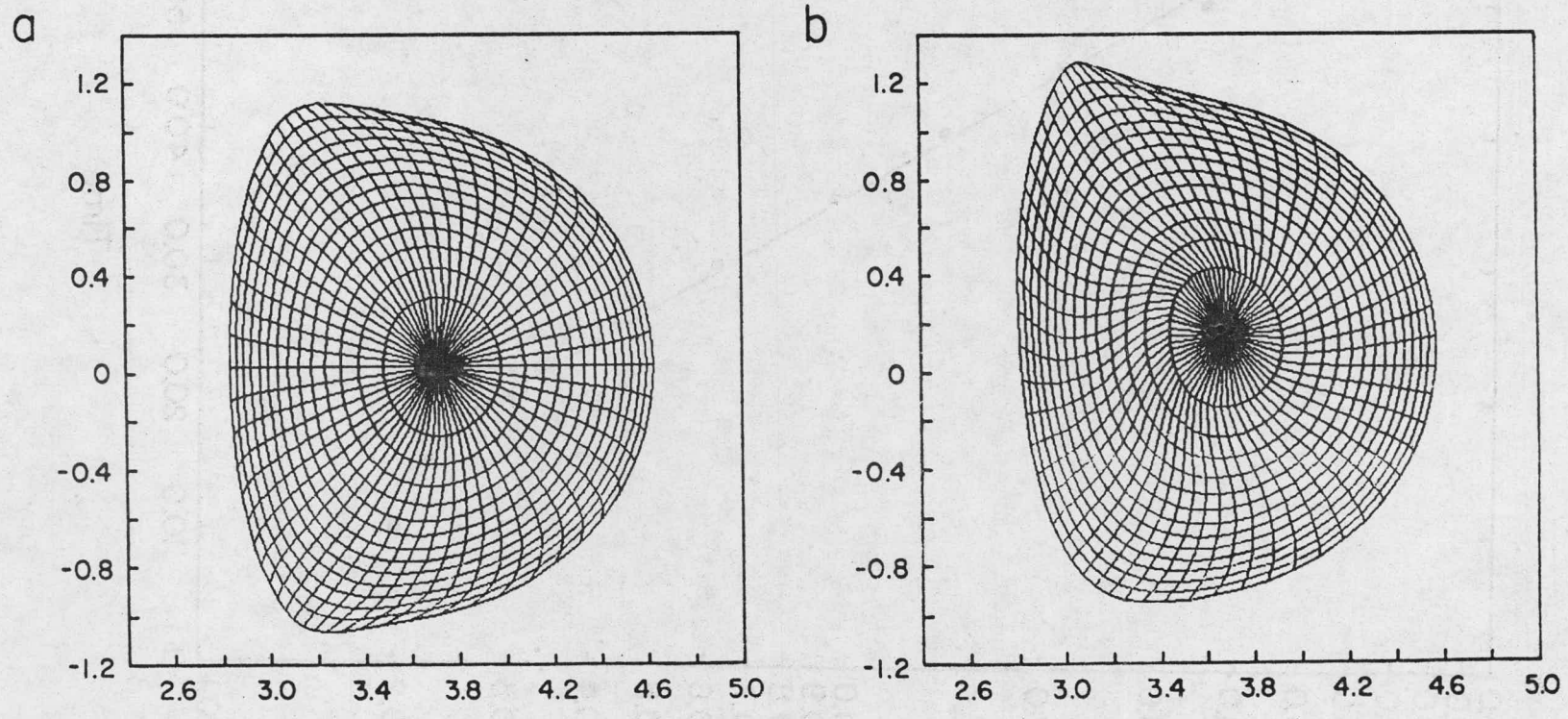

Figure 14

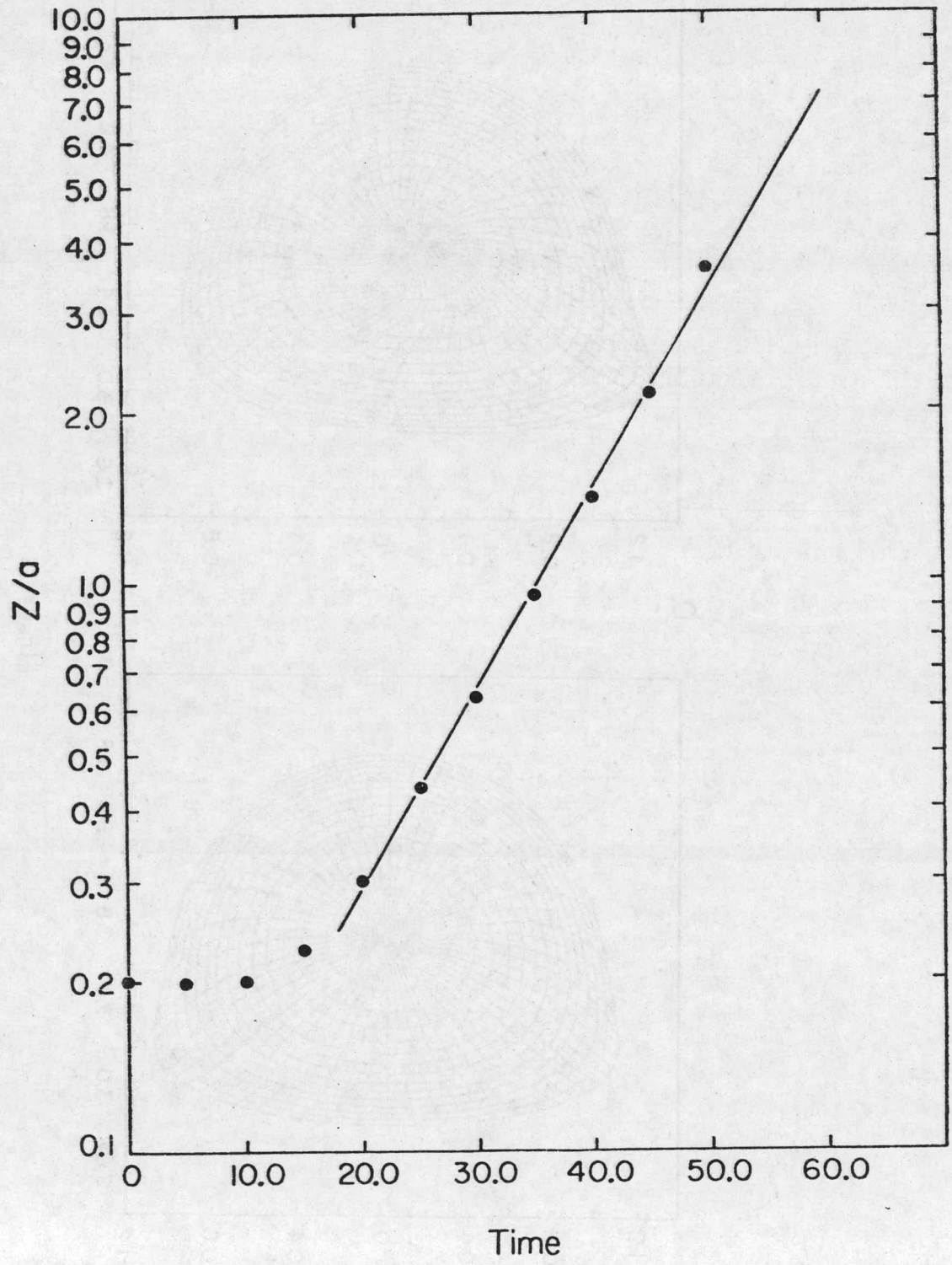
10.0
9.0
8.0
7.0
6.0
5.0
4.0
3.0
2.0
1.0
0.9
0.8
0.7
0.6
0.5
0.4
0.3
0.2
0.1
Z/a
0
10.0
20.0
30.0
40.0
50.0
60.0
Time

Figure 13

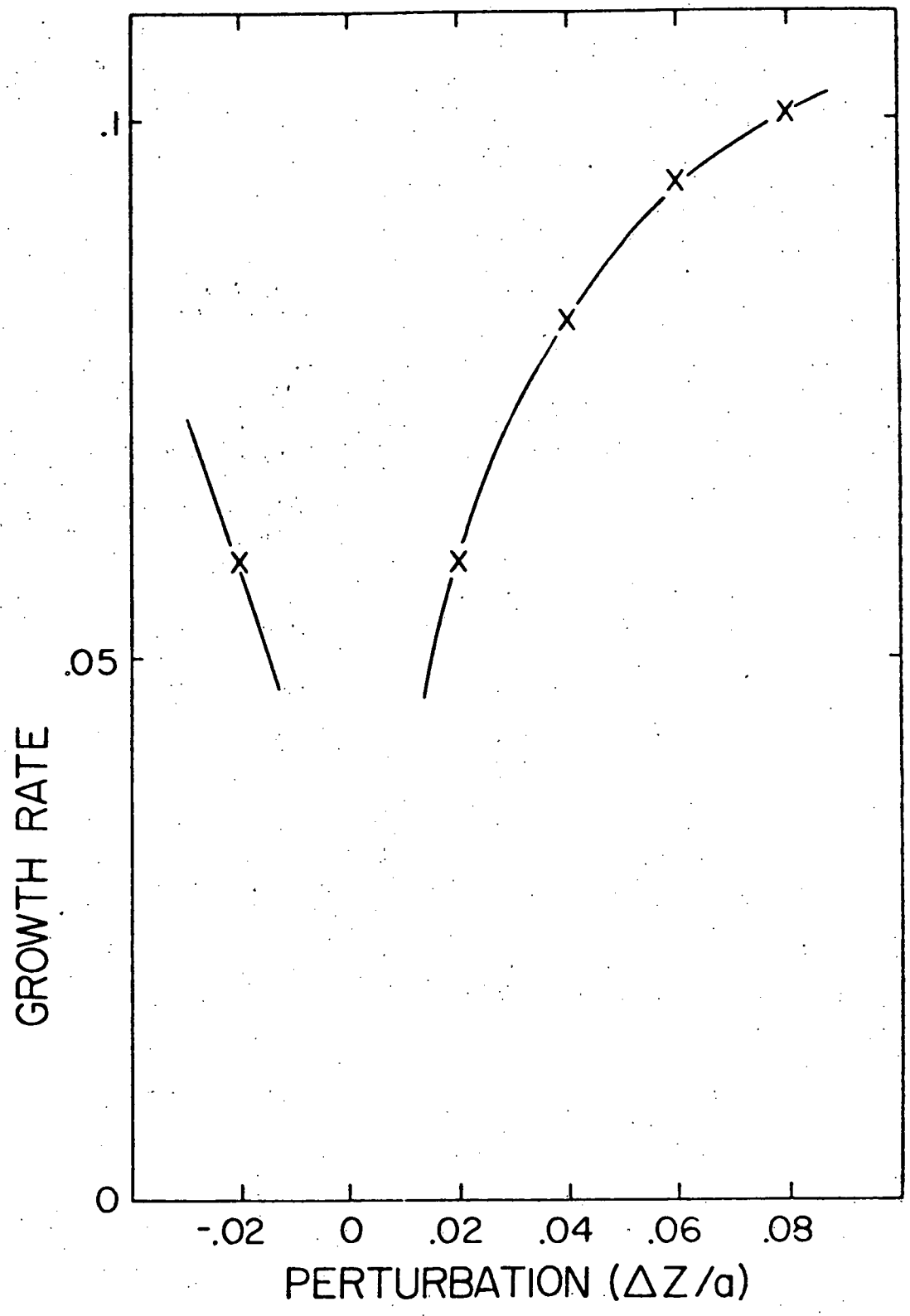

Figure 15

TABLE

THEORY	EXPERIMENT
Vertical Stability:	
Dee and inverse dee linearly unstable without feedback.	Same.
Square linearly unstable without feedback.	Linear state undetectable—square stable.
Square more stable than dee and inverse dee.	Same.
All shapes linearly stabilized by passive feedback.	Dee and inverse dee not linearly stabilized by passive feedback. All shapes can be nonlinearly stabilized by passive feedback.
$\tau_{growth} \sim \tau_{Alfvén}$, without feedback. stable, with feedback.	$\tau_{growth} \sim L/R\big\|_{plasma}$ with feedback.
Nonlinear growth is exponential.	Same.
Nonlinear motion is nonrigid, toward separatrix field null.	Same.
Effect of plasma resistivity	τ_{growth} decreases with increasing plasma resistivity which limits effectiveness of feedback.
If magnetic axis is initially placed above, below or precisely on the midplane, the plasma correspondingly moves up, down or oscillates.	Same
Horizontal Stability:	
Squarelike plasmas are more unstable than dee and inverse dee.	Same.

EXTERNAL DISTRIBUTION IN ADDITION TO UC-20

J.W. Flowers, University of Florida
H.S. Robertson, University of Miami, FL
E.G. Harris, University of Tennessee
M. Kristiansen, Texas Technical University
Plasma Research Laboratory, Australian National University, Australia
P.E. Vandenplas, Association Euratom-Etat Belge, Belgium
P. Sankanak, Institute de Fisica-Unicamp, Brazil
Mrs. A.M. Dupas, C.E.N.G., DPh-PFC-SIG, France
M.A. Layau, Centre d'Etudes Nucléaires, France
G. VonGierke, Max-Planck-Instiute Für Plasma Physic, Germany
R. Toschi, Associazione Euratom-Cnen Sulla Fusion, Cento Gas Ionizzati, Italy
K. Takayma, IPP Nagoya Imoversotu, Japan
K. Uo, Kyoto University, Japan
K. Yamamoto, JAERI, Japan
B. Lehnert, Royal Insititute of Technology, Sweden
E.S. Weibel, CRPP, Ecole Polytechnique Federale de Lausanne, Switzerland
A. Gibson, Culham Laboratory, UK
R.S. Pease, Culham Laboratory, UK
D.R. Sweetman, Culham Laboratory, UK
J.B. Taylor, Culham Laboratory, UK
D. Schuster, University of Natal, South Africa
G.M. Budker, Siberian Academy of Sciences, USSR
V.E. Golant, IOFFE Physico-Technical Institute, Academy of Sciences, Russia
I.G. Gverdtsiteli, Phisico-Tech. Inst. State Com. for Utilization of Atomic Energy, USSR
B.B. Kadomtsev, Institute of Atomic Energy, USSR
M.S. Rabinovich, Lebedev Institute, Academy of Sciences, USSR
CHeng-chung Yang, Chinese Academy of Sciences, Lanchow, Peoples Republic of China
Chi-shih Li, Chinese Academy of Sciences, Peking, Peoples Republic of China
Hsiao-wu CHeng, Chinese Academy of Sciences, Shanghai, Peoples Republic of China
Yi-chung Cho, Chinese Academy of Sciences, Peking, Peoples Republic of China
Fu-chia Yang, Futan University, Peoples Republic of China
Mei-ling Yeh, Chinese Academy of Sciences, Lanchow, Peoples Republic of China
Wei-chung Chang, Chinese Academy of Sciences, Shanghai, Peoples Republic of China
Kuei-wu Wang, Chinese Academy of Sciences, Loshan County, Peoples Republic of China
CHun-hsien CHen, Chinese Academy of Sciences, Peking, Peoples Republic of China
Li-tsien CHiu, Chinese Academy of Sciences, Peking, Peoples Republic of China
Miao-sun CHen, Chinese Academy of Sciences, Peking, Peoples Republic of China

6 for Chicago Operations Office
9 for individuals in Washington Offices

INTERNAL DISTRIBUTION IN ADDITION TO UC-20

90 for local group and file